

## Noise-induced stabilization of one-dimensional discontinuous maps

Renate Wackerbauer\*

Max-Planck-Institute for Physics of Complex Systems, 01187 Dresden, Germany

(Received 17 February 1998; revised manuscript received 13 May 1998)

Dynamical noise yields a stabilization, or switching inertia, of the flip-flop process in the Lorenz flow [R. Wackerbauer, Phys. Rev. E **52**, 4745 (1995)]. In order to understand the corresponding stabilization mechanisms in general, a systematic analysis of the influence of dynamical perturbations on the switching process of one-dimensional, discontinuous maps (a piecewise linear map, a Lorenz map, and a piecewise linear Lorenz approximation) is presented. It turns out that the dominant stabilization mechanism in all Lorenz-type maps under study is caused by a noise-induced unstable fixed point, resulting in a noise-induced escape of a typical trajectory into a less frequently visited part of the attractor. [S1063-651X(98)03909-9]

PACS number(s): 05.45.+b, 05.40.+j

### I. INTRODUCTION

The presence of small perturbations and noise, which is ubiquitous in real systems, has been the subject of various and extensive studies in nonlinear dynamical systems. In general, the effects of perturbations can be quite difficult to predict and often yield counterintuitive behavior. Even low-dimensional systems exhibit a huge variety of noise-driven phenomena, ranging from a less ordered to a more ordered system dynamics. Prominent examples are the phenomena of noise-induced chaos [1,2], noise-induced order [3], or stochastic resonance [4,5], where the signal-to-noise ratio of a periodically modulated, usually bistable system can be amplified by the addition of external noise. Furthermore, the presence of noise can alter the orbital stability in chaotic maps such that noise-induced synchronization is possible [6]. In nonhyperbolic dynamical systems, near homoclinic tangencies, noise can be amplified by the interaction with the deterministic dynamics, leading to remarkable deformations of the attractor [7].

Even in hyperbolic systems, e.g., not necessarily nonhyperbolic systems, such as the Lorenz system, which is not structurally stable but hyperbolic, noise can alter the dynamical behavior. In the flip-flop process, associated with the switching on the two symmetric lobes of the Lorenz attractor [8,9] ( $\sigma=10$ ,  $b=\frac{8}{3}$ , and  $r=28$ ), dynamical noise can stabilize the switching dynamics such that the number of successive rotations of a typical trajectory on the same lobe is significantly increased for small noise levels [10]. This noise-induced stabilization is present not only for a specific amplitude-dependent white noise, discussed in [10], but also for uniform and Gaussian white noise [11].

The present paper shows a detailed analysis of the influence of dynamical noise on switching processes in one-dimensional, discontinuous maps. On the one hand, the intention is to understand the phenomenon of noise-induced stabilization in the Lorenz system, which is why different aspects of the Lorenz system are discussed in terms of one-dimensional maps. On the other hand, different stabilization mechanisms are found which are of interest in noise-

controlled switching dynamics *per se*.

The dynamics of the Lorenz attractor is characterized by two unstable fixed points in addition to the saddle point at the origin [8,12]. A few specific features that might contribute to noise-induced stabilization characterize the antisymmetric Lorenz attractor. These features are increasing distances of successive states on any Poincaré section, a discontinuity with infinite slope that corresponds to the homoclinic orbit of the origin, and a laminar (intermittentlike) behavior near the unstable fixed points. The effect of these properties due to dynamical noise is discussed subsequently with three different one-dimensional discontinuous maps on an interval: the piecewise linear map [Eq. (4)], the Lorenz map [Eq. (5)], and a piecewise linear map exhibiting the same antisymmetric property as the Lorenz map [Eq. (6)]. It turns out that the switching dynamics of all Lorenz-type maps under study is significantly reduced by dynamical noise. This reduction is mainly caused by a noise-induced escape of a typical trajectory into a less frequently visited part of the attractor.

### II. NOISY DISCONTINUOUS MAPS

The influence of dynamical perturbations on a one-dimensional map  $F$  on the interval  $I \in \mathbb{R}$  is described by a Langevin-type equation

$$I \rightarrow I, x_i \mapsto x_{i+1} = F(x_i) + D\xi_i, \quad (1)$$

where  $\xi_i$  defines some perturbation event with amplitude  $D$ . To account for the flip-flop process in the Lorenz system, discontinuous maps are considered. Analogously to the Kramers problem of stochastic motion in a double well potential [13], the average time a trajectory spends on one branch of the attractor is called the *mean passage time*  $T$ . Throughout this paper the distance of successive states ( $x_{i+1} - x_i$ ) is called *state spacing*. For all maps  $F$  under study it is assumed that  $F(x) - x = b$  at the left boundary of the interval  $I$ , which guarantees the same minimum state spacing  $b$ .

The existence of the stabilization effect in Lorenz's system does not depend on the specific type of noise [11]. For the following analysis it is appropriate to consider random as well as regular dynamical perturbations  $D\xi_i$  in Eq. (1). (Throughout this paper, perturbations are called noise only if they stem from a stochastic process.) As random perturba-

\*Electronic address: wacker@mpipks-dresden.mpg.de

tions *uniform noise*  $\xi^{uniform}$  and *dichotomous Markov noise*  $\xi^{Markov}$  are considered. Uniform noise is defined as white  $\delta$ -correlated noise with zero mean ( $\langle \xi_i \xi_{i'} \rangle = \delta_{i,i'}$ ), where  $\xi_i$  is uniformly distributed in the interval  $\xi_i \in [-1, 1]$ . For dichotomous Markov noise,  $\xi_i$  is uniformly distributed in the set  $\xi_i \in \{-1, 1\}$ . Both types of noise are (can be) experimentally realized. From an analytical point of view, in contrast to uniform noise, dichotomous Markov noise guarantees a fixed relation of state spacing and perturbation  $\xi_i$  at any state  $x_i$ , which simplifies the analysis. Because of that, this paper deals mainly with dichotomous Markov noise. All realizations of noise sequences consist of subsequences with equal sign. The length  $l$  of such a subsequence  $\{\xi_i\}_{i=k}^{k+l-1}$  with perturbations of equal sign is defined as the *length of constant perturbations* (LCP). In addition to random perturbations, *regular perturbations*  $\xi^\varphi$  of period  $\varphi$ ,  $\varphi = 2l$ , are considered. A sequence of regular perturbations of period  $\varphi = 2$  is  $\{\xi_i\}_{i=k}^{k+5} = + - + - + -$ . The following analysis deals mainly with global dynamical noise, which means that the state of a dynamical system is homogeneously, e.g., in each iteration step, perturbed by a stochastic process. Additional stabilization can be achieved if a dynamical perturbation acts only locally in state space  $I$ , which can appear as more realistic in certain cases. This is discussed briefly below. The distinction between different dynamical perturbations ( $\xi^{uniform}$ ,  $\xi^{Markov}$ ,  $\xi^\varphi$ , global, and local) is mainly made to probe specific stabilization mechanisms. However, as a consequence of these investigations, dynamical perturbations or biased noise can be designed in order to enlarge or reduce the stabilization properties.

A further important point is the appropriate choice of the boundary correction in  $I$  as a consequence that a dynamical perturbation can throw the trajectory out of this interval. To obtain a perturbed map on the interval  $I$ , the perturbation  $\xi_i$  is set to zero whenever it would lead to a state that is not in  $I$ . Of course, this correction changes the statistics of noise, but it guarantees that the correction does not support an enlargement of the mean passage time and therefore not the existence of a stabilization phenomenon, which is consistent with the goal of this paper. (Usually, boundary corrections are chosen such that the next random noise event in the noise sequence is used for which the trajectory remains in  $I$ . In the case of dichotomous Markov noise this would mean to replace  $\xi_i$  by  $-\xi_i$  at the boundary. This is a larger correction in comparison to the replacement  $\xi_i = 0$ .) Nevertheless, the effect of this boundary correction can be estimated (Sec. IV A).

To compare perturbed and unperturbed states of a dynamical system on average for  $t=1$  and  $t=2$  time steps, the following quantities are defined:  $F^0 = F(x_i)$ ,  $F^\pm = F(x_i) \pm D$ ,  $F^{00} = F(F^0)$ , and  $F^{\pm\mp} = F(F^\pm) \mp D$ . In the trivial case, e.g., for  $t=1$  time steps, the noisy system behaves like the noiseless one because  $H^{t=1} := (F^+ + F^-)/2 - F^0 = 0$  for any map  $F$ . However, for  $t=2$  time steps, where the additive noise term interacts with the dynamical system  $F$ , the noisy dynamics is somehow faster than (equal to) the noise-free dynamics for concave (linear) maps. In this case, the corresponding quantity

$$H^{t=2} := (F^{+-} + F^{-+})/2 - F^{00} \quad (2)$$

vanishes for linear (continuous) maps and is positive for strong concave (continuous) maps if the interval  $I$  is large enough such that the dynamics is not influenced by boundary corrections or discontinuities. This seems to be in contradiction to a stabilization property and directs focus on the interaction of perturbations with discontinuities. Notice that the above arguments still hold if  $+ -$  and  $- +$  in Eq. (2) are replaced by  $++$  and  $--$ .

### Symbolic dynamics and entropy

The switching dynamics (flip-flop process) of a discontinuous map under study is described as a symbolic dynamical system. Thereby the state space  $I$  is partitioned with respect to the discontinuity at  $x=d$  into two cells, which are represented by the symbols 0 and 1. Then a typical trajectory  $\{x_i\}_{i=0}^\infty$  can be mapped to a symbol sequence  $S = \{s_i\}_{i=0}^\infty$ , such that a symbol 0 (1) is assigned to  $s_i$  if a state  $x_i$  is on the left (right) side of the discontinuity ( $s_i = 0$  for  $x_i < d$  and  $s_i = 1$  for  $x_i > d$ ). The corresponding symbolic dynamical system [14] is defined as  $\Sigma_F \rightarrow \Sigma_F$ , and  $S \mapsto \hat{\sigma}_F(S) = S'$  such that any symbol in the sequence  $S$  fulfills  $s_{i+1} = s'_i = \hat{\sigma}_F(s_i)$ .  $\Sigma_F$  is the space of all admissible symbol sequences, e.g., sequences that are induced by the dynamical system for all initial states  $x_0$  on the attractor. The operator  $\hat{\sigma}_F$  is called *shift operator on  $\Sigma_F$*  and describes the dynamics generated by  $F$  in the space of symbol sequences  $\Sigma_F$ . For practical purposes the length  $L$  of a symbol sequence, defined by  $S = \{s_i\}_{i=0}^{L-1}$ , is regarded as finite. A word  $A_{j,n}$  of length  $n$ ,  $A_{j,n} \in \{s_k s_{k+1} \dots s_{k+n-1} | k=0, 1, \dots, L-n\}$ , represents the set of sequences (trajectories) that coincide in the first  $n$  successive symbols. The set of admissible words  $P_n$ ,  $P_n = \{A_{j,n}\}_{j=1}^N$ , consists of all words of length  $n$  that appear in the sequence  $S$ ; it is called  *$n$ -cylinder-induced partition  $P_n$* .

In this paper the complexity of the symbol sequences on a finite time scale  $n$  is quantified by the (block) entropy  $K(n)$  [15]:

$$K(n) = \frac{-\sum_{j=1}^N p_j \log p_j}{n}, \quad (3)$$

where  $p_j$  is the probability that a given word  $A_{j,n}$  of length  $n$  appears in the symbol sequence  $S$  and  $\log$  represents the binary logarithm.

In the following analysis, binary sequences of length  $L = 10^6$  and words of length  $n=4$  are considered.  $n=4$  is of the order of the typical time scale  $T(D=0)$  of the switching processes.

### III. OBVIOUS EFFECT: STABILIZATION BY LOCAL NOISE

#### The piecewise linear map

The piecewise linear map [Eq. (4)] is characterized by a linear increase of the state spacing and a discontinuity with fixed threshold at  $x=d$ :

$$F: [0,1] \rightarrow [0,1], x_i \mapsto x_{i+1} = (ax_i + b) \bmod_1. \quad (4)$$

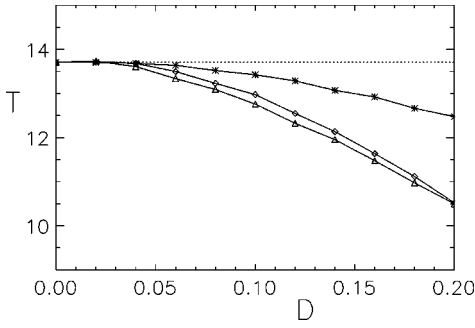


FIG. 1. Mean passage time  $T$  for the piecewise linear map [Eq. (4), with  $a=1.05$  and  $b=0.05$ ] versus the noise level  $D$ : uniform noise (\*), dichotomous Markov noise ( $\diamond$ ), and regular perturbations with period  $\varphi=2$  ( $\triangle$ ).

With the chosen parameters of  $a=1.05$  and  $b=0.05$  the minimum state spacing is  $F(0)=0.05$ .

Figure 1 shows the influence of dynamical perturbations on the switching behavior: The mean passage time  $T$  (mean number of states on  $[0,d)$ ) decreases with noise level  $D$  for all considered perturbations and reflects that noise-induced stabilization does not exist for this linear discontinuous map.  $T$  is larger for uniform noise than for dichotomous Markov noise because  $\langle |\xi_i^{\text{uniform}}| \rangle = \langle |\xi_i^{\text{Markov}}| \rangle / 2$ , whereas the behavior of dichotomous Markov noise  $\xi^{\text{Markov}}$  and regular dynamical perturbation  $\xi^{\varphi=2}$  is very similar. As already pointed out, the linearity of  $F$  far from the discontinuity leads to  $H^{t=2}=0$  [Eq. (2)] and therefore does not explain the decrease of  $T$ . However, a discussion of  $H^{t=2}$  near the discontinuity [16] shows that the discontinuity at  $x=d$  leads to a decrease of  $T$  as soon as  $D > 1-d$  on the unit interval  $I$ , where  $1-d$  is the maximum state spacing of  $F$  on  $I$ . For the considered parameters  $a=1.05$  and  $b=0.05$  the discontinuity appears at  $d=0.905$  and the decrease of  $T$  is expected for  $D > 0.095$ . This is in good agreement with Fig. 1 because  $T$  shows a more steep decline with increasing  $D$  in the neighborhood of this critical noise level  $D_c=0.095$ . The small decrease of  $T$  with  $D$ , already for  $0.05 < D < D_c$ , reflects the influence of the boundary correction at  $x=0$ , where the state spacing takes its minimum value of 0.05.

In contrast to global dynamical noise, local dynamical noise can lead to a considerable switching inertia (enlargement of  $T$ ) even for linear maps. This is demonstrated in Fig. 2, where the dependence of the mean passage time  $T$  on the noise level  $D$  is plotted for  $a=1.05$  and different minimum state spacings  $b=0.01$  ( $0.001$ ). In the case where noise is added in each iteration step, one gets a reduction of switching with increasing  $D$  as discussed above. In contrast, if noise is added locally, for example, on the subinterval  $[0.2,0.8]$ , the mean passage time  $T$  is clearly increasing with  $D$ . This is caused by the asymmetry of the state spacing on the left and right boundaries of this subinterval together with the fact that noise can throw a trajectory out of the subinterval, but not back into it. Assuming a negative noise event at the left boundary  $x=0.2$ , the corresponding trajectory performs a loop in such a way that  $x_i=0.2-D$  and  $x_{i+i_m} \geq 0.2$ , where  $i_m$  is the minimum number of iterations fulfilling this condition. For a state  $x_i=0.8$ , a positive noise event lets the trajectory jump to  $x'_i=0.8+D$  by jumping over the

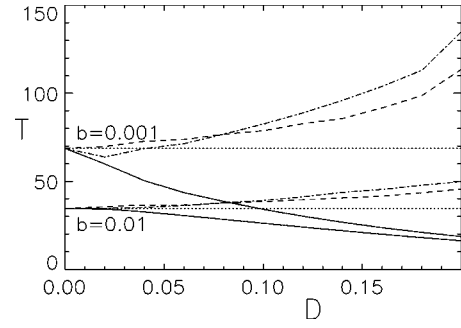


FIG. 2. Mean passage time  $T$  versus noise level  $D$  for the piecewise linear map ( $a=1.05$ ,  $b=0.01$ , and  $b=0.001$ ): local noise on  $[0.2,0.8]$  (dot-dashed line), the corresponding approximation by  $T(D=0) + i_m - i_p$  (see the text, dashed line), and global noise (full line). The dotted lines correspond to the noise-free mean passage time  $T(D=0)=34.4$  for  $b=0.01$  and  $T(D=0)=79.3$  for  $b=0.001$ .

states  $x_{i+i_p}$ , where  $i_p$  is the minimum number of iterations fulfilling  $x_{i+i_p} \leq 0.8+D$ . Thus, as a rough approximation, a trajectory gains  $i_m$ ,  $i_m > i_p$ , discrete states and loses  $i_p$  states per passage, whereby  $H^{t=2}=0$  within the interval. This reason for stabilization is confirmed in Fig. 2 by comparing the graph of  $T(D=0) + i_m - i_p$  with the graph for local noise.

Thus local noise in state space can clearly support the stabilization effect if the state spacing is not constant, even in cases where there is no stabilization for global noise. One consequence, from an analytical point of view, is that any stabilizing effect of dynamical noise on specific local features of maps cannot be investigated by considering local noise since local noise superimposes an additional stabilization mechanism on the noisy switching dynamics. This is why a discussion of local noise, in order to understand noise-induced stabilization in the Lorenz map, is avoided within this paper. Furthermore, this type of noise can be regarded as realistic or interesting to consider also from an experimental point of view, when different subprocesses of a dynamical system are perturbed by noise with different strength.

#### IV. FORMATION OF NOISE-INDUCED UNSTABLE FIXED POINTS

##### A. The Lorenz map

Studying geometric models of the Lorenz flow by one-dimensional maps of an interval onto itself has led to a remarkable understanding of the Lorenz system, for example, the bifurcation behavior at homoclinic explosions, at preturbulence, or at the Hopf bifurcation [12,17]. The interaction of dynamical perturbations with the deterministic dynamics of the Lorenz attractor ( $\sigma=10$ ,  $b=8/3$ , and  $r=28$ ) is discussed by means of the corresponding Lorenz map (Fig. 3) [12,17]

$$F: [-1,1] \rightarrow [-1,1],$$

$$x_i \mapsto x_{i+1} = \begin{cases} 1 - \beta |x_i|^\alpha, & x_i \in [-1,0) \\ 0, & x_i = 0 \\ -1 + \beta |x_i|^\alpha, & x_i \in (0,1] \end{cases} \quad (5)$$

and the corresponding standard parameters  $\alpha=1/\beta+0.001$  and  $\beta=1.95$ . The minimum state spacing at  $|x|=1$  is  $1 - F(1)=0.05$ .

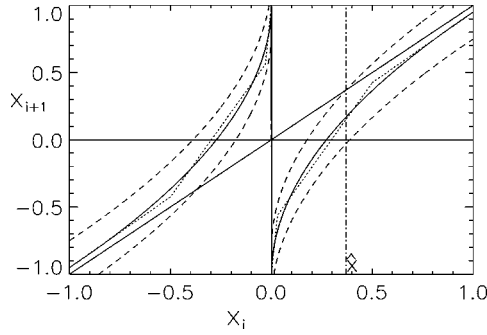


FIG. 3. Lorenz map (full line), a linear approximation (dotted line), and the noisy Lorenz map ( $D=0.2$ , dashed line).

The analysis of the noisy Lorenz map and Lorenz-type maps focuses on the block entropy, which appears as a more promising quantity than the mean passage time  $T$  alone, for the understanding of the stabilization mechanisms. As seen in Fig. 4(a), the entropy  $K$  decreases with increasing noise level  $D$  for random dynamical perturbations (uniform noise and dichotomous Markov noise), reflecting a more inhomogeneous distribution of words in the corresponding symbol sequences in the perturbed case. A more detailed investigation of the distribution of words shows that the probability of finding a constant word in the symbol sequence is  $p('0000') + p('1111') = 0.29$  (0.35) for dichotomous Markov noise with amplitude  $D=0.1$  (0.2), in comparison to the noise-free case, where  $p('0000') + p('1111') = 0.23$ . This reflects that constant words are more frequent in the noisy symbol sequence and that a noisy trajectory stays longer on the same branch of the attractor. This effect is called noise-induced stabilization [10] and is also expressed in an increase of the mean passage time  $T$  of 8% (20%) for  $D=0.1$  (0.2) in Fig. 4(b). In contrast to that, for regular dy-

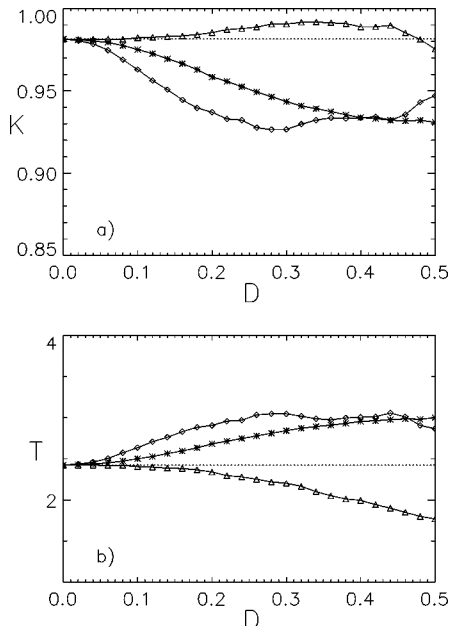


FIG. 4. (a) Entropy  $K(n=4)$  and (b) mean passage time  $T$  versus noise level  $D$  for the Lorenz map: uniform noise (\*), dichotomous Markov noise ( $\diamond$ ), and regular perturbations with period  $\varphi=2$  ( $\triangle$ ).

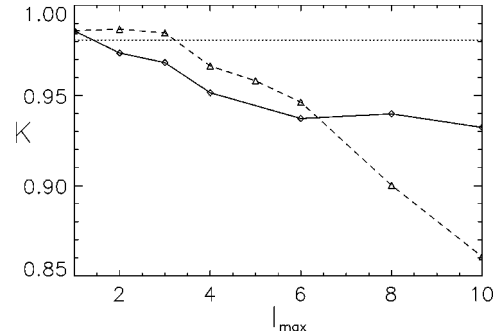


FIG. 5. Entropy  $K(n=4)$  versus maximum length of constant perturbations  $l_{max}$  for dynamical perturbations with amplitude  $D=0.2$ : dichotomous Markov noise (full line) and regular perturbations  $\varphi=2l_{max}$  (dashed line). The dotted line corresponds to  $D=0$ .

namical perturbations  $\xi^{\varphi=2}$ , no stabilization is present. The dynamics is characterized by a small increase in the entropy  $K$  and a decrease in the mean passage time  $T$  with noise level  $D$ , although the dynamical states are perturbed by the same amplitude of “noise”  $D$ . For large noise amplitudes, near  $D>0.4$ , the random process dominates the switching dynamics and, correspondingly, the frequency of constant words starts shrinking, which is reflected in Figs. 4(a) and 4(b).

One important difference between dichotomous Markov noise and regular perturbations is the maximum LCP  $l_{max}$ . For the considered regular perturbation it is  $l_{max}=\varphi/2=1$ , whereas for the considered realization of dichotomous Markov noise it is  $l_{max}=15$ . The average LCP for  $\xi^{Markov}$  is  $\langle l \rangle = 2.0$ , in comparison to the mean passage time  $T(D=0)=2.4$ . A more detailed analysis [16] shows that the noise-induced entropy reduction, e.g., the stabilization property, decreases if the maximum LCP is successively reduced in the noise sequence  $l_{max}=15, 10, 8, \dots, 1$ . This is represented in Fig. 5 for a specific noise amplitude  $D=0.2$ .

The noise-induced switching inertia is also reflected in the probability distribution of the states of a typical trajectory that is plotted in Fig. 6(a) for the noise-free case as well as for dichotomous Markov noise and regular perturbations  $\xi^{\varphi=2}$  with noise amplitude  $D=0.2$ . A noiseless trajectory ( $D=0$ ) is more frequently near the discontinuity  $x_i=0$  than near  $x_i=1$ . This remains true for the regular dynamical perturbation  $\varphi=2$ . However, for dichotomous Markov noise the probability of a trajectory near  $x_i=0$  is reduced, whereas the probability of states  $x_i>0.6$  is clearly increased. Both features express the stabilization property that might be caused by two different effects, discussed below. [Because of the antisymmetry  $F(-x)=-F(x)$  of the map, only switching from the left to the right branch is discussed throughout this paper, without losing universality.]

In the first mechanism noise changes the distribution of switching states. Thereby, a state  $x_i$  is called switching state if it switches in the next time step  $i+1$  from the left to the right branch. It is defined by  $x_{i-1}<0$  and  $x_i>0$ . From the dynamical behavior of the Lorenz map in Fig. 3 it follows that if an orbit comes close to the discontinuity for  $x_i<0$ , the following state (switching state) is close to the end point  $x_i=1$  and the number of iterations on the right branch is maximal. Thus, if noise changes the distribution of switching states such that states close to  $x_i=1$  are more frequent, the

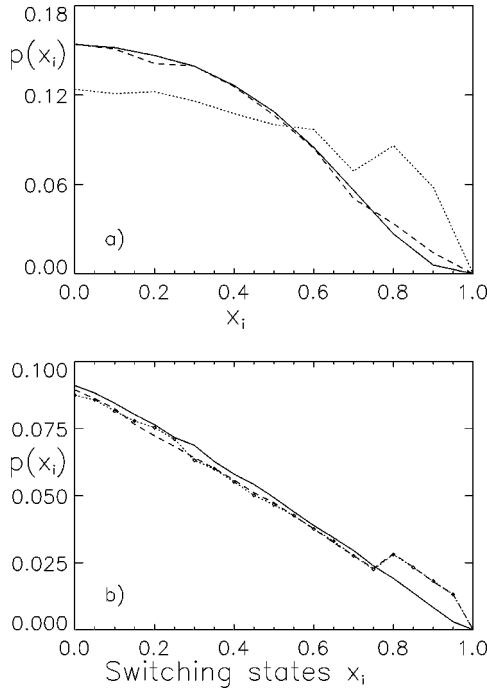


FIG. 6. Probability distribution of (a) all states and (b) the switching states:  $D=0$  (full line), dichotomous Markov noise ( $D=0.2$ , dotted line), and regular perturbations  $\xi^{\nu=2}$  ( $D=0.2$ , dashed line).

mean passage time might be increased. In Fig. 6(b) the distributions of switching states for the noise-free orbit and for perturbed orbits (regular and random perturbations,  $D=0.2$ ) are compared with each other. All graphs coincide approximately, except for  $x_i > 0.8$ , where an increased probability in *both* perturbed cases shows that a dynamical perturbation can throw the trajectory out from the interval  $I$ . A combination of the two facts that (i) the probability of switching states with  $x_i > 0.6$  is the same for both perturbed cases [Fig. 6(b)] and (ii) the stabilization effect vanishes for regular dynamical perturbations, indicates that this first argument is not the dominating one for explaining noise-induced stabilization in the Lorenz map.

In the second mechanism noise induces an unstable fixed point. As a consequence of the noise-induced unstable fixed point  $\tilde{x}$  of  $F+D$ , which exists in  $I$  for noise levels  $D > 0.05$  (Fig. 3), the existence of an attractive region  $\mathcal{A} = [\tilde{x}, 1] \subset I$  of the map  $F+D$  is generated. Here, the LCP is explicitly taken into account, since for  $x_+ < x_i < 0^-$ , where  $F(x_+) + D = \tilde{x}$ , a noise subsequence  $\{\xi_i\} = ++(+ \dots)$  directs the orbit into the attractive region  $\mathcal{A}$ . There the direction of iteration is reversed for positive noise events  $\xi_i > 0$  in comparison to the noise-free case, which is a necessary condition for the escape of a trajectory. Notice the similarity of the noisy map  $F \pm D$  to the Lorenz map in the parameter regime near and at the existence of preturbulence [18,12].

Since mainly subsequences with constant perturbations are responsible for the stabilization phenomenon, one expects that driving forces with an increased frequency of such subsequences might further enlarge the stabilization. This is the case for colored noise, but especially for periodic perturbations. For this last case, the decrease of entropy with the

maximum LCP,  $l_{max} = \varphi/2$ , is plotted in Fig. 5 for  $D=0.2$ . Stabilization is present as soon as  $\varphi/2$  is of the order of the typical time scale  $T(D=0)$  of the switching process. In comparison to dichotomous Markov noise the stabilization effect is more marked for  $l_{max} > 6$  in the case of regular perturbation because perturbations with  $l > 6$  are more frequent in periodic sequences than in realizations of random noise.

The effect of the boundary correction on the mean passage time  $T$  can be estimated by comparing the values of  $T$ , calculated with and without boundary correction. For dichotomous Markov noise and no boundary correction near the noise-induced fixed points,  $T$  increases continuously with the noise amplitude  $D$ . Without (with) boundary correction one finds an increase of  $T=40\%$  (20%) for  $D=0.2$  and  $T=110\%$  (20%) for  $D=0.4$  in comparison to the noise-free case. For regular perturbations ( $\varphi=2$ ),  $T$  remains constant without boundary correction, independent of the noise level  $D$ .

This identified stabilization mechanism in the discrete-time system can be transferred directly to the continuous-time Lorenz system, where stabilization was reported earlier [10,11]. There the first component of the Lorenz system was perturbed by different types of noise, steadily after some stroboscopic time. Although the comparison can be only qualitatively, it is obvious that also in the continuous case, noise can induce or better shift the two symmetric unstable fixed points such that a typical trajectory is able to come closer to (escape into the direction of) the noise-free unstable fixed points. The decrease in the entropy value is about the same for the time-continuous and the time-discrete system.

## B. The piecewise linear Lorenz map

A linear approximation of the Lorenz map in Eq. (5) by two linear functions per branch is defined as piecewise linear Lorenz map

$$F: [-1,1] \rightarrow [-1,1],$$

$$x_i \mapsto x_{i+1} = \begin{cases} f_1(x_i), & x_i \in [-1,0) \\ 0, & x_i = 0 \\ f_2(x_i) = -f_1(-x_i), & x_i \in (0,1], \end{cases} \quad (6)$$

with  $f_1(0^-) = 1$  and  $f_1(x_i) = ax_i + b$  for  $-1 \leq x_i < \kappa < 0$  and  $a > 1$ . The parameter  $b$  is fixed as  $b = a - 0.95$  in order to have the same minimum state spacing as in the Lorenz map  $f_1(-1) + 1 = 0.05$ . This map can be regarded as a generalization of the Lorenz map, since it exhibits the same symmetry, but allows us to vary the length of the laminar phase ( $\kappa$ ) and the corresponding slope  $a$ . A further advantage is that critical noise levels for different stabilization mechanisms can be derived analytically. Although this map exhibits a rich variety of dynamical behavior for different parameters, it is discussed in close connection to the Lorenz map in the following. In particular, the linear approximation of the Lorenz map in Fig. 3, consisting of two kinks (at  $\kappa_1 = -0.2$ ,  $\kappa_2 = -0.03$ ), is discussed in detail by the piecewise linear Lorenz map [Eq. (6)] with only one kink per branch (located at  $\kappa$ ). This allows us to focus on the influence of dynamical noise on both kinks separately and therefore to simulate different aspects of the Lorenz map separately. (Because of the

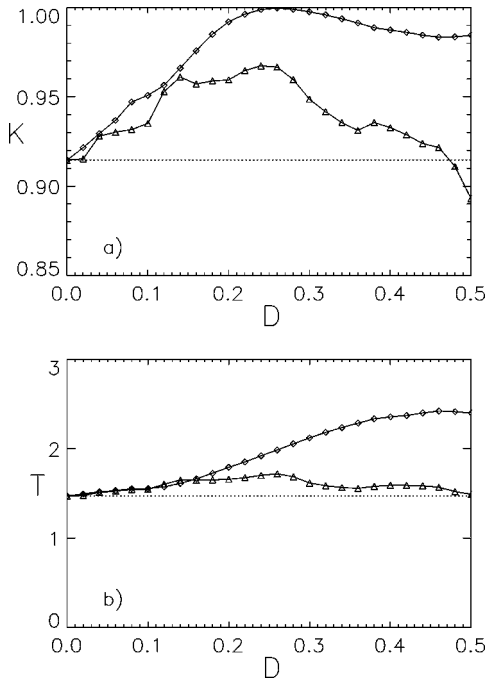


FIG. 7. (a) Entropy  $K(n=4)$  and (b) mean passage time  $T$  versus noise level  $D$  for the piecewise linear Lorenz map ( $\kappa = -0.03$ ): dichotomous Markov noise ( $\diamond$ ) and regular perturbations with period  $\varphi=2$  ( $\triangle$ ).

antisymmetric property of this map, again, only switching from the left to the right branch is discussed, without losing universality.)

### 1. Approximation in the neighborhood of the discontinuity: $\kappa = \kappa_2$

To study the effect of dynamical noise in the Lorenz map near the discontinuity, where the slope tends to infinity, the parameters in Eq. (6) are chosen as  $\kappa = \kappa_2 = -0.03$  and  $a = 1.56$ , such that the piecewise linear Lorenz map coincides with the approximation of the Lorenz map in Fig. 3 for  $|x_i| < |\kappa|$ . In Fig. 7 noise-induced stabilization is quantified by (a) the entropy  $K(n=4)$  and (b) the mean passage time  $T$ : The entropy increases with  $D$  for  $D < 0.26$ , whereas for larger noise levels, the entropy decreases [Fig. 7(a)]. The mean passage time  $T$  increases with the noise level  $D$  near  $D < 0.16$  for both dichotomous Markov noise and regular perturbations ( $\varphi=2$ ). For larger amplitudes  $D$  both graphs split, indicating a change in the underlying mechanism for noise-induced switching inertia:  $T$  still increases for dichotomous Markov noise, whereas  $T$  remains constant for regular perturbations. Similarly to the Lorenz map, two stabilization mechanisms can be identified, which are discussed below.

The first mechanism is a redistribution of switching states. In the noise-free case the distribution of switching states is characterized by a step at  $x_i = f_1(\kappa)$ , where  $f_1(\kappa) = 0.56$  for the considered parameters (Fig. 8). This step is caused by a comparatively large slope of the map for  $|x_i| < \kappa$ , and this is why the support of the attractor can be divided in one subset  $I_1 = [-D - f_1(\kappa), f_1(\kappa) + D]$ , which is visited often by the trajectory, and the complementary subset  $I_2 = I - I_1$ , which is less frequently visited. For the noise-free case and  $x_i \in I_1$ , only passages of one or two iterations per

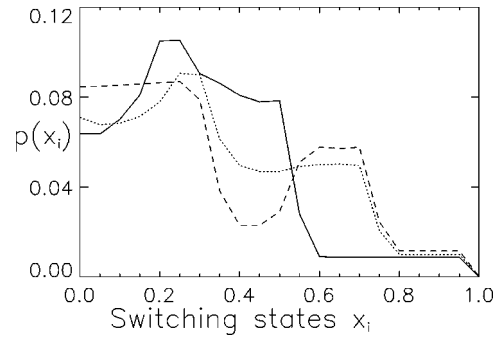


FIG. 8. Probability distribution of the switching states for  $D=0$  (full line), dichotomous Markov noise ( $D=0.2$ , dotted line), and regular perturbations  $\xi^{\varphi=2}$  ( $D=0.2$ , dashed line).

branch are possible [16]. This is reflected in the probability distribution of words of length  $n=4$  such that it is dominated by words “0101” and “0110” and the corresponding symmetric ones. Correspondingly, the mean passage time is small,  $T(D=0) = 1.5$ , as is the entropy value.

Dynamical perturbations lead to a redistribution of switching states in the interval  $\tilde{I}_1 = [f_1(\kappa) - D, f_1(\kappa) + D] \in I_1$ , whereas for  $x_i > f_1(\kappa) + D$  the graphs nearly coincide for both noisy and the noise-free cases (Fig. 8). This redistribution of switching states allows more iterations per passage with increasing noise level  $D$  for some  $x_i \in \tilde{I}_1$  since the upper boundary of  $\tilde{I}_1$  increases. A more detailed discussion in [16] shows that this gain of states dominates the loss of states that is caused by a decrease of the lower boundary of  $\tilde{I}_1$ . For  $D > 0$ , the corresponding probability distribution of words is characterized by an increase of words of type 0110 and 0111, respectively, and, in parallel, a reduction of the most frequent words 0101. Thus the entropy as well as  $T$  increases slowly for  $D > 0$  (Fig. 7).

The second mechanism is the existence of a noise-induced unstable fixed point. For noise levels larger than the minimum state spacing,  $D > 0.05$ , the existence of an unstable fixed point  $\tilde{x}$ ,  $\tilde{x} = (b - D)/(a - 1)$ , of the map  $f_2 + D$  on  $I$  yields the existence of an attractive region  $\mathcal{A} = [\tilde{x}, 1] \subset I$ . Thus, as soon as a trajectory visits  $\mathcal{A}$ , positive perturbations can direct the trajectory to the end point. For small noise amplitudes  $D$ , the probability of a trajectory to visit  $\mathcal{A}$ , is small since  $I_1 \cap \mathcal{A} = \{ \}$ . However, as soon as a critical noise level  $f_1(\kappa) + D > \tilde{x}$  is reached, e.g.,  $D > D_{\mathcal{A}}$  and  $D_{\mathcal{A}} = 0.19$  for the considered parameters, this probability is clearly increased because  $I_1 \cap \mathcal{A} \neq \{ \}$ . Then a trajectory can escape into  $I_2$ , the less frequently visited subset of the attractor, already for frequent switching states  $x_i \in I_1$ , because  $I_2 \subset \mathcal{A}$ . (In principle, this mechanism is the same as for the Lorenz system, except that the arguments are more quantitative and critical parameters can be calculated analytically.)

The effect of the second stabilization mechanism is demonstrated in the distribution of words ( $n=4$ ) in Fig. 9. For  $D = 0.16$ , which is below the critical noise level  $D_{\mathcal{A}} = 0.19$ , the distribution is dominated by words of type 0101 and on a minor part by words of type 0110. Near  $D = 0.22 \approx D_{\mathcal{A}}$ , a transition to a rather homogeneous distribution takes place; the corresponding entropy takes its maximum value of about

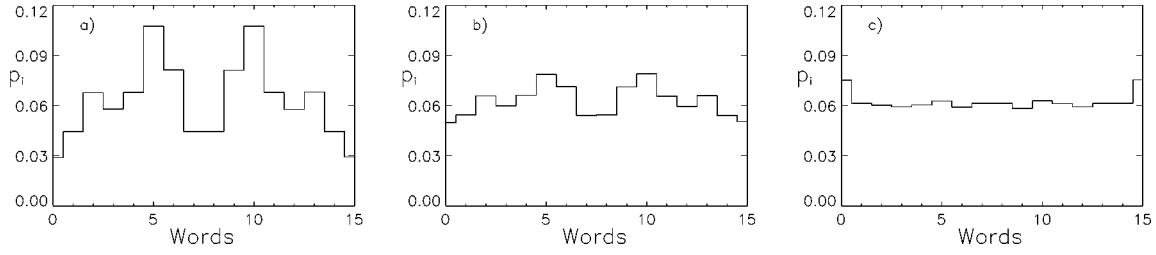


FIG. 9. Probability distribution of words of length  $n=4$  (a) below ( $D=0.16$ ), (b) near ( $D=0.22$ ), and (c) above ( $D=0.28$ ) the critical noise level  $D_A=0.19$ . The words are represented by their normalized binary number representation.

$K(n=4)=1$  and remains constant. Above the critical noise level  $D > D_A$  ( $D=0.26$ ), constant words are dominant in the distribution of words, yielding again a structured distribution and therefore a decrease in the entropy.

Again, as a consequence of the second stabilization mechanism, regular perturbations with period  $\varphi=2l$  and  $l=1,2,4,6,8,10$  enlarge the mean passage time by 10%, 14%, 60%, 83%, 123%, and 157%, in comparison to dichotomous Markov noise, where the corresponding factor is 47% for  $D=0.3$ . It is further remarkable that both stabilization mechanisms are visible in the entropy graph [Fig. 7(a)], but they become obvious in the  $T$  graph only if different types of perturbations are considered [Fig. 7(b)].

## 2. Approximation in the neighborhood of the laminar phase: $\kappa=\kappa_1$

The approximation of the Lorenz map near the laminar phase is studied in two cases: (i)  $\kappa=-0.2$ , for which stabilization is clearly marked, and (ii)  $\kappa=-0.5$ , which is more relevant for the Lorenz map (Fig. 3). In both cases ( $a=1.05$ ), the piecewise linear Lorenz map coincides with the approximation of the Lorenz map in Fig. 3 for  $|x_i| > |\kappa|$ . In contrast to the preceding subsection, both kinks are located at  $\kappa < f_1^{-1}(0^-)$ . Thus their influence on the trajectory is earlier than the time step immediately before switching. This results in an amplification of the noise level that is superimposed on the two stabilization mechanisms and is discussed below.

For the kink at  $\kappa=-0.2$ , the piecewise linear map  $f_1$  is given by  $f_1(x_i)=1.05x_i+0.1$  for  $x_i \leq \kappa$  and  $f_1(x_i)=5.55x_i+1$  for  $x_i \geq \kappa$ . The entropy  $K(n=4)$  decreases with the noise level  $D$  (Fig. 10) and reflects the existence of a noise-driven stabilization. In contrast to the previous case, the sta-

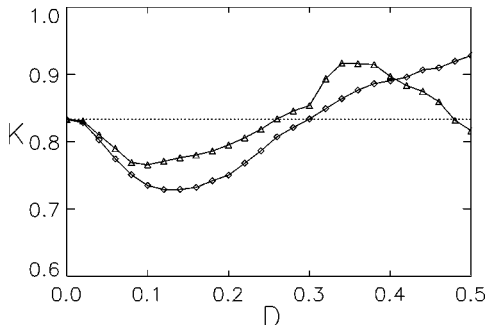


FIG. 10. Entropy  $K(n=4)$  versus noise level  $D$  for the piecewise linear Lorenz map ( $\kappa=-0.2$ ): dichotomous Markov noise ( $\diamond$ ) and regular perturbations with period  $\varphi=2$  ( $\triangle$ ).

bilization effect appears for smaller noise levels and is present even for regular perturbations ( $\varphi=2$ ). For  $D=0.1$ , the mean passage time  $T$  is enlarged by 23% for regular perturbations ( $\varphi=2$ ), in comparison to 45% for dichotomous Markov noise.

The first mechanism is a redistribution of switching states. For the noise-free case, the distribution of switching states in Fig. 11 is characterized by a step at  $x_i=f_1^2(\kappa)=0.39$ . The less frequently visited subset of the attractor  $I_2=[f_1^2(\kappa),1]$  is determined by the second iterate of  $f_1$  since a trajectory with  $x_i=\kappa$  stays on the left branch for two more time steps because  $\kappa < f_1^{-1}(0^-)$  and  $f_1^2(\kappa) > 0$ . As a consequence, the corresponding redistribution of switching states on  $\tilde{I}_1$  for  $D > 0$  (Fig. 11) is governed by an effective noise level, which is larger than the true noise level. For dichotomous Markov noise the interval is given by  $\tilde{I}_1^{Markov}=[f_1(f_1(\kappa)-D)-D, f_1(f_1(\kappa)+D)+D]$ , which can be rewritten as  $\tilde{I}_1^{Markov}=[f_1^2(\kappa)-D_{eff}^{Markov}, f_1^2(\kappa)+D_{eff}^{Markov}]$  and an effective noise level  $D_{eff}^{Markov}$ . For the piecewise linear Lorenz map, this effective value is given by  $D_{eff}^{Markov}=(m+1)D$ , where  $m$  is the slope of  $f_1$  for  $x_i > \kappa$ , e.g.,  $D_{eff}^{Markov}=6.5D$  for the considered parameters. This amplified noise level fits well with the distribution of switching states in Fig. 11. For regular perturbations ( $\varphi=2$ ), the corresponding interval  $\tilde{I}_1^{\varphi=2}$  is slightly smaller because  $\tilde{I}_1^{\varphi=2}=[f_1(f_1(\kappa)-D)+D, f_1(f_1(\kappa)+D)-D]$ . This corresponds to an effective noise level of  $D_{eff}^{\varphi=2}=(m-1)D$ , yielding  $D_{eff}^{\varphi=2}=4.5D$  for the considered parameters. In both cases, dynamical perturbations are amplified by the interaction with the dynamical system and therefore stabilization is present even for regular perturbations.

The second mechanism is the existence of a noise-induced unstable fixed point. This mechanism leads to additional stabilization for dichotomous Markov noise as well as for regular perturbations with periods  $\varphi > 2T(D=0)$ , whereby the time scale of the noise-free system is  $T(D=0)=4.3$ . However, the critical noise level  $D_A=0.06$  is considerably small than Sec. IV B 1, reflecting the strong amplification of noise.

The shape of the graphs in Fig. 10 are determined by two additional effects [16]. First, near  $D > 0.1$ , the entropy starts growing with noise level  $D$  for  $\xi^{Markov}$  as well as for  $\xi^{\varphi=2}$ : This is caused by the fact that states  $x_i < \kappa$  exist such that the first iterate is a switching state  $f_1(x_i)+D > 0$ . This happens as soon as  $f_1(\kappa)+D > 0$ , e.g.,  $D > 0.11$ . The second remark concerns the decrease of the entropy with noise level  $D$  for  $D > 0.35$ , only for regular perturbations  $\xi^{\varphi=2}$ . This is caused by a rapid increase of words 0101 and reflects that the tra-

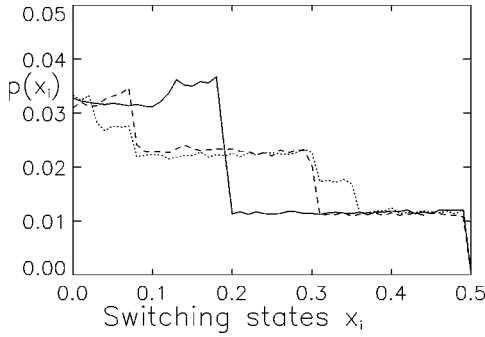


FIG. 11. Probability distribution of the switching states for  $D=0$  (full line) for dichotomous Markov noise ( $D=0.05$ , dotted line) and regular perturbations  $\xi^{\nu=2}$  ( $D=0.05$ , dashed line).

jectory can be captured near the discontinuity for this particular type of regular perturbation, not discussed in more detail.

For the kink at  $\kappa=-0.5$ , for the piecewise linear Lorenz map with  $\kappa=-0.5$ , the corresponding step in the distribution of switching states for  $D=0$  is less marked in comparison to  $\kappa=-0.2$  because the slope for  $x_i>\kappa$  is reduced,  $m=2.85<5.5$ . Thus the redistribution of switching states by dynamical noise with respect to the noise-free case is smaller for  $\kappa=-0.5$ . As a consequence, the stabilization property is nearly vanishing for regular perturbation as seen in Fig. 12. The maximum stabilization is 8% for  $D=0.06$  and regular perturbations  $\xi^{\nu=2}$  and 21% for  $D=0.1$  and dichotomous Markov noise.

Otherwise, for  $\kappa=-0.5$ , noise is amplified by two dynamical interactions because  $f_1^2(\kappa)=-0.21$  and  $f_1^3(\kappa)=0.40$ . The corresponding amplification of, for example, positive noise events, is given by  $(1+m+m^2)D$ , e.g.,  $12D$  for  $m=2.85$ , and is about two times larger than for the case  $\kappa=-0.2$ . This strong amplification of noise causes a more steep increase of  $T$  near  $D=0$  for  $\kappa=-0.5$  (Fig. 12) than it is the case for  $\kappa=-0.2$ . Furthermore, it yields also a small critical noise level  $D_A=0.05$  for the onset of the second stabilization mechanism that dominates the degree of stabilization.

The specific choice of the kink at  $\kappa=-1$  corresponds to a single piecewise approximation of the Lorenz map on  $I$ . Although noise-induced stabilization still exists in this case, it becomes significantly visible in the corresponding graphs ( $K$ ,  $T$ ) only, after some proper techniques are applied.

### 3. Comparison with the Lorenz map

For the piecewise linear Lorenz map, in both cases ( $\kappa=-0.03$  and  $\kappa=-0.5$ ) two mechanisms for noise-driven stabilization are found: (i) noise-induced redistribution of the switching states, corresponding to an enlargement of the frequently visited part of the attractor, and (ii) noise-induced unstable fixed point, corresponding to a possible escape of a trajectory to the endpoints  $|x_i|=1$ . In addition, for  $\kappa=-0.5$ , an amplification of noise ( $D_{eff}>D$ ) is superimposed on these two processes, which leads to a shift of the stabilization phenomenon to smaller noise levels as demonstrated in Fig. 12 for  $\kappa=-0.03$  and  $\kappa=-0.5$ .

Additionally, Fig. 12 represents the stabilization effect for the Lorenz map and for its two-kink approximation (Fig. 3).

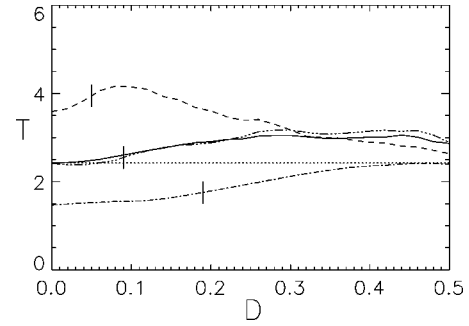


FIG. 12. Comparison of the mean passage time  $T$  versus noise level  $D$  (dichotomous Markov noise) for different approximations of the Lorenz map: —, Lorenz map; ···, linear approximation with two kinks ( $\kappa_1=-0.5, \kappa_2=-0.03$ ), and piecewise linear Lorenz map for  $\kappa=-0.5$  (—) and  $\kappa=-0.03$  (·-·-). The vertical ticks mark the corresponding critical noise levels  $D_A$  and the dotted line marks  $T(D=0)$  for the Lorenz map.

This approximation is defined by  $f_1(x_i)=1.05x_i+0.1$  for  $x_i<-0.5$ ,  $f_1(x_i)=2.1x_i+0.625$  for  $-0.5\leq x_i<-0.03$ , and  $f_1(0^-)=1$  on the left branch of  $I$  and reproduces noise-induced stabilization in the Lorenz map (Fig. 12). The dependence of the mean passage time  $T$  on the noise level  $D$  for the Lorenz map and its two-kink approximation is similar to the behavior of the piecewise linear Lorenz map for  $\kappa=-0.03$ , but shifted to smaller noise levels. This shift results from a smaller critical noise level  $D_A=0.09<0.19$ , calculated analytically for the two-kink approximation from  $f_1(-0.03)+D_A=\tilde{x}$ . This critical value  $D_A=0.09$  determines exactly the noise level where stabilization becomes obvious for the Lorenz map, as seen in Fig. 12, supporting the hypothesis that the second mechanism is the dominant one.

The time scale of the flip-flop processes is different in both maps:  $T(D=0)=2.4$  for the Lorenz map and its two-kink approximation and  $T(D=0)=1.5$  for the piecewise linear Lorenz map ( $\kappa=-0.03$ ). For the Lorenz map, constant words of length  $n=4$  are already dominant for  $D=0$ , in contrast to the piecewise linear Lorenz map, where switching 0101 dominates. Increasing  $D$  in the first case increases the frequency of constant words for small  $D$ . Thus entropy does not increase with  $D$  ( $D$  small) for the Lorenz map in Fig. 4, in contrast to the piecewise linear Lorenz map in Fig. 7.

## V. CONCLUSIONS

To understand noise-induced stabilization (NIS) in the Lorenz system [10], the influence of dynamical perturbations (uniform white noise, dichotomous Markov noise, and regular perturbations) on the switching dynamics of one-dimensional discontinuous maps is discussed. For the piecewise linear system (modulo discontinuity) a stabilization (enhancement of the mean passage time) is present if noise is added locally in state space, which is in contrast to global noise, where no stabilization is found. For the Lorenz map as well as for piecewise linear approximations, exhibiting the same antisymmetric property as the Lorenz map, stabilization is present even for global noise, as it is the case in the three-dimensional Lorenz flow. A detailed analysis shows that this stabilization is mostly caused by the existence of a



noise-induced unstable fixed point, yielding a noise-induced attractive region of the state space and resulting in an intermittent escape of the trajectory into a less frequently visited subset of the attractor. This stabilization can be clearly enhanced if regular (colored) perturbations with periods longer than two times the typical time scale of the noiseless system are considered.

The identified stabilization mechanisms with respect to one-dimensional maps can be transferred directly to the three-dimensional Lorenz flow to related switching processes in other continuous dynamical systems, but of course also to other one-dimensional discontinuous maps. For example, consider Lorenz-type maps with smoothed kinks or corresponding maps with modulo discontinuity. However, a generalization of the phenomenon of NIS to one-dimensional discontinuous maps is not possible since in particular cases either stabilizing or destabilizing [16] factors can dominate the perturbed switching dynamics.

From a methodical point of view, it is demonstrated by a comparative analysis of the mean passage time and the block entropy, based on a symbolic dynamical description of the switching process, that additional information can be extracted from the output signal by means of the entropy. This supports that symbolic dynamics is a promising concept for the analysis of switching dynamics, as already pointed out by

Witt, Neimann, and Kurths [19] and others in the context of stochastic resonance.

The most prominent effect with respect to noise-driven switching processes is stochastic resonance (SR) [4]. Although its notion has a very broad meaning in the literature, it is claimed that NIS under study is not a SR phenomenon, either in the conventional meaning of signal amplification [4] or in generalized versions such as aperiodic stochastic resonance [20] or noise-free SR [21,22], since all these realizations of SR show a minimum in the mean passage time at a certain noise level. However, several properties found in the noisy Lorenz system (map) are related to findings in the transient dynamics of an overdamped particle in a noisy cubic potential [23] or in a noisy bistable system operating in the strong forcing regime [24,25]. These properties are postponed switch events or enhancement of stabilization by colored noise. This motivates a detailed comparative analysis of both types of noisy switching processes.

#### ACKNOWLEDGMENTS

I would like to thank H. Kantz and W. Just for helpful discussions and for carefully reading the manuscript. I am also very grateful to J. Yorke for stimulating discussions.

- 
- [1] G. Mayer-Kress and H. Haken, *J. Stat. Phys.* **26**, 149 (1981).
  - [2] I.I. Fedchenia, R. Mannella, P.V.E. McClintock, N.D. Stein, and N.G. Stocks, *Phys. Rev. A* **46**, 1769 (1992).
  - [3] S. Rajasekar, *Phys. Rev. E* **51**, 775 (1995).
  - [4] *J. Stat. Phys.* **70** (1993), special issue on stochastic resonance, edited by A. Bulsara, P. Hänggi, F. Marchesoni, F. Moss, and M. Shlesinger.
  - [5] V.A. Shneidman, P. Jung, and P. Hänggi, *Phys. Rev. Lett.* **72**, 2682 (1994).
  - [6] G. Malescio, *Phys. Lett. A* **218**, 25 (1996).
  - [7] L. Jaeger and H. Kantz, *Physica D* **105**, 79 (1997).
  - [8] E.N. Lorenz, *J. Atmos. Sci.* **20**, 130 (1963).
  - [9] F. Aicardi and A. Borsellino, *Biol. Cybern.* **55**, 377 (1987).
  - [10] R. Wackerbauer, *Phys. Rev. E* **52**, 4745 (1995).
  - [11] R. Wackerbauer (unpublished).
  - [12] C. Sparrow, *The Lorenz Equations: Bifurcations, Chaos, and Strange Attractors* (Springer, New York, 1974), Vol. 41.
  - [13] H.A. Kramers, *Physica* **7**, 284 (1940).
  - [14] V.M. Alekseev and M.V. Yakobson, *Phys. Rep.* **75**, 287 (1981).
  - [15] R. Wackerbauer, A. Witt, H. Atmanspacher, J. Kurths, and H. Scheingraber, *Chaos Solitons Fractals* **4**, 133 (1994), and references therein.
  - [16] R. Wackerbauer, Max Planck Institute, Report No. MPIP/KS/9802009, 1998 (unpublished).
  - [17] J. Guckenheimer and P. Holmes, *Nonlinear Oscillations, Dynamical Systems and Bifurcation of Vector Fields* (Springer, New York, 1983).
  - [18] J.L. Kaplan and J.A. Yorke, *Commun. Math. Phys.* **67**, 93 (1979).
  - [19] A. Witt, A. Neimann, and J. Kurths, *Phys. Rev. E* **55**, 5050 (1997).
  - [20] J.J. Collins, C.C. Chow, A.C. Capela, and T.T. Imhoff, *Phys. Rev. E* **54**, 5575 (1996).
  - [21] V. Anishchenko, A. Neimann, and M. Safanova, *J. Stat. Phys.* **70**, 183 (1993).
  - [22] E. Reibold, W. Just, J. Becker, and H. Benner, *Phys. Rev. Lett.* **78**, 3101 (1997).
  - [23] I. Dayan, M. Gitterman, and G.H. Weiss, *Phys. Rev. A* **46**, 757 (1992).
  - [24] R.N. Mantegna and B. Spagnolo, *Phys. Rev. Lett.* **76**, 563 (1996).
  - [25] F. Apostolico, L. Gammaitoni, F. Marchesoni, and S. Santucci, *Phys. Rev. E* **55**, 36 (1997).